

# Investigation of Dynamic Behaviour of Double Feed Induction Generator and Permanent Magnet Synchronous Generator Wind Turbines in Failure Conditions

Huseyin Calik\*<sup>‡</sup>, Ahmet Dabakoglu \*\*, Yuksel Oguz\*\*\*

\* Electrical and Electronics Engineering, Engineering Faculty, Giresun University, Gaziler, 28200 Giresun, Turkey

\*\* Electrical and Electronics Engineering, Institute of Graduate Studies, Istanbul University–Cerrahpasa, Avcilar, 34320 Istanbul, Turkey

\*\*\* Electrical and Electronics Engineering, Technology Faculty, Afyon Kocatepe University, ANS Kampüsü Gazlıgöl Yolu, 03200, Afyonkarahisar, Turkey

(huseyin.calik@giresun.edu.tr, ahmet.dabakoglu@ogr.iu.edu.tr, yukseloguz@aku.edu.tr)

<sup>‡</sup> Corresponding Author; First Author, Electrical and Electronics Engineering, Engineering Faculty, Giresun University, Gaziler, 28200 Giresun, Turkey, Tel: +90 454 310 1740,  
Fax: +90 545 310 17 49, huseyin.calik@giresun.edu.tr

*Received: 02.03.2021 Accepted:17.04.2021*

**Abstract-** The variable nature of the wind significantly affects the generation of electrical energy and integrating large power wind farms into the grid can cause electrical quality problems. The increase in the number of wind turbines connected to the grid is resulting in electricity quality problems including voltage instability and difficulties in reactive power and frequency control. This study investigates the resilience of two forms of wind turbine, the permanent magnet synchronous generator (PMSG) and double-feed induction generator (DFIG), to disturbances that may occur in the network, such as symmetrical and non-symmetric short circuit conditions, and voltage drops. Models of PMSG and DFIG wind turbines have been developed in the MATLAB-Simulink environment and simulated operating at nominal power level for the same network conditions and wind speed. The simulation was then used to investigate the dynamic response of the wind turbines in the case of phase-ground, phase-phase-ground, and three-phase-ground short circuit failure, and voltage fluctuations, in order to determine which generator system has greatest benefit for electrical power quality. The DFIG wind turbine system was found to reach nominal active power faster than the PMSG wind turbine system. In addition, the frequency converter for the PMSG wind turbine system was more affected by failures in the power grid resulting in excessive DC bus voltages.

**Keywords** PMSG; DFIG; Fault Ride Through FRT, LFRT; Low Voltage Ride Through, VRT; Wind Turbine Generators.

## 1. Introduction

Developments in wind turbine technology in the last decades have increased their capacity rapidly and they have become widely used. However, connecting wind farms with high power capacity to the grid presents problems that relate to electrical quality such as voltage drop, flicker, and harmonics [1]. In order to reduce the problems associated with electrical quality when wind turbines are connected to the grid, transmission system operators have introduced

many regulations that require wind turbines to comply with standards for voltage and frequency in the network and behavior under fault conditions [2-3]. In the event of a short circuit or voltage drop, the performance of a wind turbine should be verified to ensure that it meets the requirements specified by the regulations [4].

The impact of a turbine connected to the grid is closely related to the type of generator and the type of connection to

the grid. Wind turbines transfer varying amounts of power to the grid depending on the state of the wind. In order to avoid the disturbances this causes, the desired reactive power should be supplied to the network and the voltage should be balanced. The increase in the proportion of wind turbines compared to other power sources connected to the grid causes an increase in the negative effects of turbines on the network [5]. The large-scale integration of Wind Power Plants (WPPs) may have harmful impact on the grid, as they are considered intermittent power sources. Therefore, interconnection requirements for WPPs are being developed worldwide to mitigate their negative impact and protect the reliability of the power grid [6–7]. Today much research focuses on Low Voltage Ride Through (LVRT) capability of a WPP, and has been studied in recent years considering unbalanced and distorted grid conditions [8-9].

Fault Ride Through (FRT) capability can be defined as the ability of a wind turbine to remain connected to the power grid during fault conditions and provide support to the grid [10]. Grid regulations provide the control of the FRT capacity of facilities, and the active and reactive power that is supplied to the network from the power plants [4].

FFT-based methods are commonly used to determine power quantities such as RMS voltage, power factor, active and reactive power, and provide useful information for a SCADA system of WPPs. The FFT requires the signal to be periodic in nature, and only provides accurate assessment in steady state [10-11]. However, a WPP may introduce a low voltage at the point of interconnection (POI) caused by a power system fault [8,12], as might occur during unbalanced or distorted grid conditions. In addition, harmonics are injected into the grid by the variable speed of WPPs due to the switching of the power electronic converters. Therefore, from the perspective of the electrical grid, WPPs are perceived as fluctuating power sources and can best be described as non-stationary, non-sinusoidal, and unbalanced in nature [13-14]. In order to enhance the LVRT capability of a WPP, the low RMS voltage at the POI caused by a power system fault should be assessed accurately. Under such conditions, the signal becomes aperiodic, and the frequency content of the signal changes with time. Hence, FFT-based methods will provide erroneous results when there are real-world disturbances [15-16]. The application of time-frequency analysis TFA in wind power has been demonstrated in the research work of [15-17]. Also, in [15-17] TFA-based analysis of instantaneous THD is used to analyze the impact of wind power in the grid. The method defines THD to be based on the ratio of the energy of the fundamental to energy of the harmonic components instead of using RMS values. Nonetheless, [15-17] provide inaccurate assessment of the impact of wind power on the grid [15].

The first wind turbines used in power generation were permanent magnet synchronous generators (PMSG) connected directly to the grid. Pitch control is applied in wind turbines to limit the mechanical power in the rotor blades that may occur due to the wind speed. Therefore, the first models were created for this type of wind turbine. Due to the variable nature of wind, modern wind turbines use a

dual-feed induction generator (DFIG) with a power electronics interface that controls the rotor current required to capture maximum energy in variable winds.

Models for wind farms provide insight into the performance of systems against the distortion and failure conditions of the grid and are important to provide information on power quality. In this study, the behavior of DFIG and PMSG wind turbines against short circuit conditions and voltage drop are investigated and their dynamic response is compared.

## 2. Modeling the Wind Turbines

The mechanical power of a wind turbine is given by Equation 1:

$$P_W = \frac{1}{2} \rho \pi R^2 V_W^3 C_p(\lambda, \beta) \quad (1)$$

Where:

$P_W$  = power obtained from the wind

$\rho$  = air density

$R$  = blade radius

$V_W$  = wind speed

$C_p$  is the power factor of the wind turbine and is defined as the nonlinear function of the tip speed ratio,  $\lambda$ , and blade pitch angle,  $\beta$ , and is given in Equation 2:

$$C_p = \frac{1}{2} * (\lambda - 0.022 * \beta^2 - 5.6) * e^{-0.17\lambda} \quad (2)$$

Where:

$$\lambda = \frac{V_W}{\omega_B}$$

$\omega_B$  = rotational speed of the turbine.

The theoretical maximum value for the power factor is  $C_p = 0.593$  and this value is called the Betz limit. The effect on the power factor  $C_p$  for varying values of  $\lambda$  and for different values of  $\beta$  (stepped by 2 deg.) is shown in Fig. 1. The blue line represents  $C_p$  for  $\beta = 0$  deg. and is the maximum value of  $C_p$ . Fig. 2 shows how the characteristics of the wind turbine vary with wind speed, starting from the nominal value and increasing  $\beta$  by steps of 2 deg.

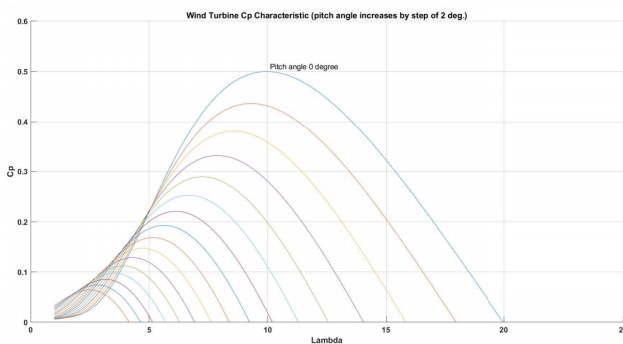


Fig. 1.  $C_p - \lambda$  curves for different angle  $\beta$

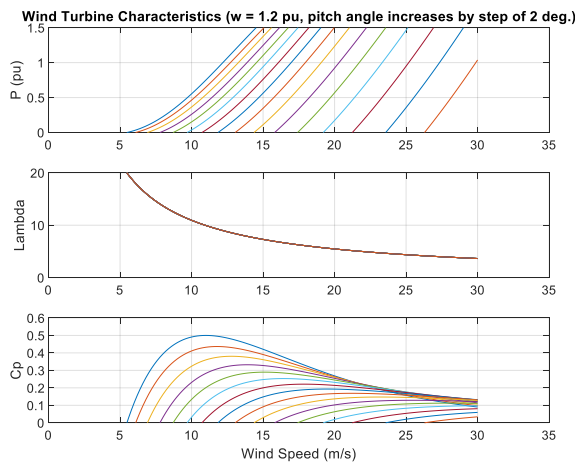


Fig. 2. Wind turbine characteristics

### 2.1. Modeling of Double-Feed Induction Generator (DFIG) Wind Turbines

The DFIG wind turbine consists of gear box, rotor side filter, back to back converter circuit, grid side filter, generator, and transformer circuit [18]. The circuit model of the DFIG is shown in Fig. 3.

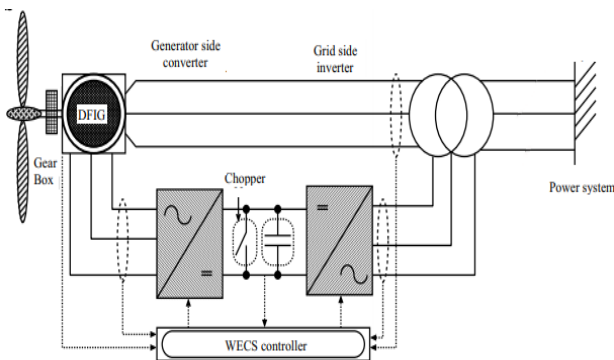


Fig. 3. DFIG wind turbine

The DFIG is directly connected to the grid via the stator, but the rotor can be connected to the grid via a converter and a filter [19]. Back to back inverters located in the DC bus section enable the DFIG to operate at variable speeds. Stator and rotor voltage equations for DFIG are given in Equation 3 and 4:

$$V_S = R_S I_S + \frac{\partial \vartheta_S}{\partial t} + j\omega_S \vartheta_S \quad (3)$$

$$V_R = R_R I_R + \frac{\partial \vartheta_R}{\partial t} - j\omega \vartheta_R \quad (4)$$

Where:

$R_S, R_R$  = stator and rotor resistance

$\vartheta_S, \vartheta_R$  = stator and rotor flux

$\omega_S$  = synchronous frequency.

$\omega_S, \omega_R$  = stator and rotor angular velocities.

The slip frequency is given in Equation 5:

$$\omega = \omega_S - \omega_R \quad (5)$$

The DFIG equations may be expressed as a two-phase axes set as given in Equation 6:

$$\left. \begin{aligned} V_{Sd} &= R_S I_{Sd} + \frac{\partial \vartheta_{Sd}}{\partial t} - \omega_S \vartheta_{Sq} \\ V_{Sq} &= R_S I_{Sq} + \frac{\partial \vartheta_{Sq}}{\partial t} + \omega_S \vartheta_{Sd} \\ V_{Rd} &= R_R I_{Rd} + \frac{\partial \vartheta_{Rd}}{\partial t} - \omega_R \vartheta_{Rq} \\ V_{Rq} &= R_R I_{Rq} + \frac{\partial \vartheta_{Rq}}{\partial t} + \omega_R \vartheta_{Rd} \\ \vartheta_{Sd} &= (L_{IS} + L_M) I_{Sd} + L_M I_{Rd} \\ \vartheta_{Sq} &= (L_{IS} + L_M) I_{Sq} + L_M I_{Rq} \\ \vartheta_{Rd} &= (L_{IR} + L_M) I_{Rd} + L_M I_{Sd} \\ \vartheta_{Rq} &= (L_{IR} + L_M) I_{Rq} + L_M I_{Sq} \end{aligned} \right\} \quad (6)$$

Where:

$L_M$  = mutual inductance

$L_S$  and  $L_R$  = stator and rotor leakage inductances.

In most practical work, the DFIG has a unitless conversion rate  $n$ . This should be included in the leakage flux relations. In addition, the magnetic flux of the d and q axes must be defined.

### 2.2. Modeling Permanent Magnet Synchronous Generator (PMSG) Wind Turbines

Power converters are required to operate variable speed PMSG wind turbines in synchronization with the voltage and frequency of the electrical grid. A PMSG wind turbine will be connected to the electricity grid via a converter able to manage its maximum power. Figure 4 shows the block diagram of a PMSG. In this type of wind energy conversion system, the PMSG wind turbine stator terminals are connected to the power grid via a two-step power conversion system AC-DC-AC, with coupling filter and step-up transformer [20].

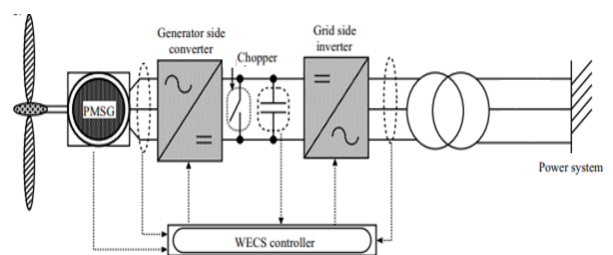


Fig. 4. PMSG wind turbine

The dynamic model of PMSG is represented as the d magnetic flux axis with respect to the two-phase synchronous reference frame, and the q axis is 90° ahead of the d axis with respect to the direction of rotation.

$$\frac{\partial I_d}{\partial t} = \frac{V_d}{L_d} - \frac{RI_d}{L_d} + \frac{L_q}{L_d} p\omega_R I_q \quad (7)$$

$$\frac{\partial I_q}{\partial t} = \frac{V_q}{L_q} - \frac{RI_q}{L_q} + \frac{L_d}{L_q} p\omega_R I_d - \frac{\psi p\omega_R}{L_q} \quad (8)$$

$$T_{el} = \frac{3}{2} p [\psi I_q + L_{dq} I_d I_q] \frac{RI_d}{L_d} + \frac{L_q}{L_d} p\omega_R I_q \quad (9)$$

Where:

$L_q, L_d$  = q and d axes inductances

$R$  = stator winding resistance

$I_d, I_q, V_d, V_q$  = q and d axes currents and voltages

$\psi$  = flux amplitude induced in the stator phases by permanent magnets

$p$  = number of pole pairs

$T_{el}$  = electromagnetic torque.

All values are calculated by reducing the rotor circuit to the stator.

### 3. Grid Integration and Failure Cases

Although wind power is one of the fastest growing industries in the world, electricity generation depends entirely on wind speed; any fluctuation in wind speed will affect the production of wind energy, making integration of wind turbines into the grid a challenging process. Design problems must be resolved, in addition to any maintenance or operating issues. In order to overcome such problems, grid operators issue grid regulations and wind farms must comply with these regulations to maintain the stability of the grid. In this way, wind power plants and conventional power plants, which differ in behavior, may be combined in the network, ensuring the continuity of energy supply. To ensure that electricity is safely distributed to end users via the grid, each country specifies its technical requirements in its grid regulations. Power generation and distribution parties in an open electricity market must meet the technical requirements determined by the relevant institution [21].

Although PMSG is generally preferred in wind turbine systems isolated from the grid, as the magnetization source is not externally provided, the full-size inverter and battery management circuits make the system complex and costly [22]. DFIG systems, on the other hand, are increasingly being seen in isolated wind systems due to their ability to maintain stator voltage and frequency stable at the desired level and can be used with a one-way inverter [23].

With the increasing use of wind energy systems, the process of connection to the grid has gained greater importance. Sudden changes in the wind have a significant effect on the

amount of power that can be obtained, and thus the effect on the grid stability. Fault Ride Through (FRT) allows the wind farm to remain connected to the grid, rather than isolating from the grid during voltage drop, and provides voltage stabilization by providing reactive power. FRT is also needed in cases of sudden voltage drop, unstable or large load changes, as a result of short circuit failure in the grid. FRT behavior for generation facilities is regulated by grid regulations [24].

### 4. Wind Turbine System Modelling

This section describes the simulation of DFIG and PMSG wind turbines to determine behavior during fault conditions for two wind farm topologies. The DFIG and PMSG wind farm models are given in Fig. 5 and Fig. 6.

During the simulation, the phase-neutral voltage of the wind turbines is monitored to determine the voltage and the active and reactive power in the generator output busbar to determine the maximum value and behavior during short circuit failure and voltage drop.

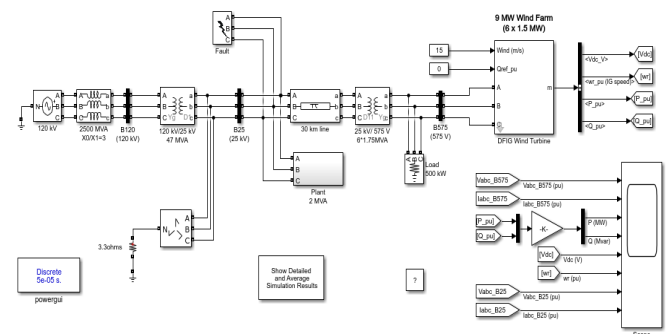


Fig. 5. DFIG wind farm simulation model.

The behavior of the wind power plants and grid are investigated for the following conditions with a constant wind speed of 15 m/s:

- Normal operating conditions
- 1-phase-ground fault
- Phase-phase-ground fault
- 3-phase-ground fault
- Grid voltage drop from 1pu to 0.5pu

The Simscape Power Systems package of MATLAB/Simulink program is used for simulation. Simulation time is set to duration sufficient to show all transient behavior, and was typically 25 or 30 seconds.

In the simulation, the generator output voltage is set as 575 V, the medium voltage transmission line as 25 kV, and the high voltage transmission line as 120 kV. A 575 V/25 kV 12 MVA transformer is connected to the medium voltage

busbar. A 500 kW load is placed at the output of the generator. The output of the transformer is connected to the grid with a 10 km medium voltage transmission line. An induction motor with 2 MVA, 1.68 MW, 2300 V voltage and power factor of 0.93, and a facility containing a 200 kW resistive load is connected to the 25 kV busbar. There is an earthing transformer to form a neutral point in the medium voltage network. The medium voltage busbar is connected to the high voltage line with a conversion ratio of 25 kV/120 kV and a 47 MVA transformer. The same model was created for the PMSG wind farm. The system parameters are summarized in Table 1.

**Table 1** System parameters

Generator Type	DFIG	PMSG
Nominal Wind speed (m/s)	15	
Rated line to line Voltage (V <sub>rms</sub> )	575	
Rated Power (MW)	9	10

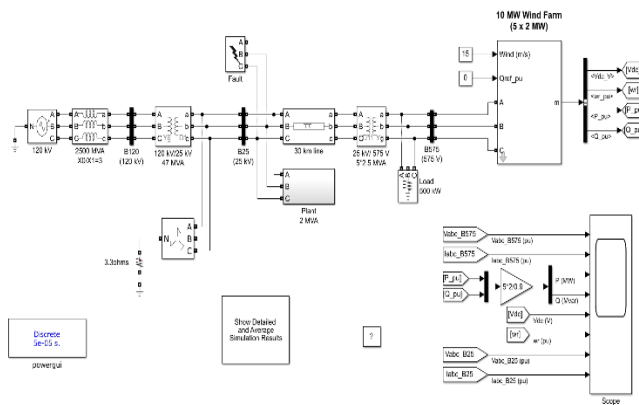


**Fig. 6.** PMSG wind farm simulation model.

**5. Results**

The behavior of the DFIG and PMSG wind turbines under normal operating conditions are given in Fig. 7 and 8 respectively and show that the wind turbine and grid voltages quickly stabilize to nominal values. The same parameters are compared in the dynamic responses to short circuit failure and voltage fluctuations.

Fig. 9 and Fig. 10 show the behavior of the wind power plants and the grid under the conditions of constant wind speed and 1-phase-earth fault. Both types of wind turbine exhibit transients during the period of the earth fault but retain stable behavior.

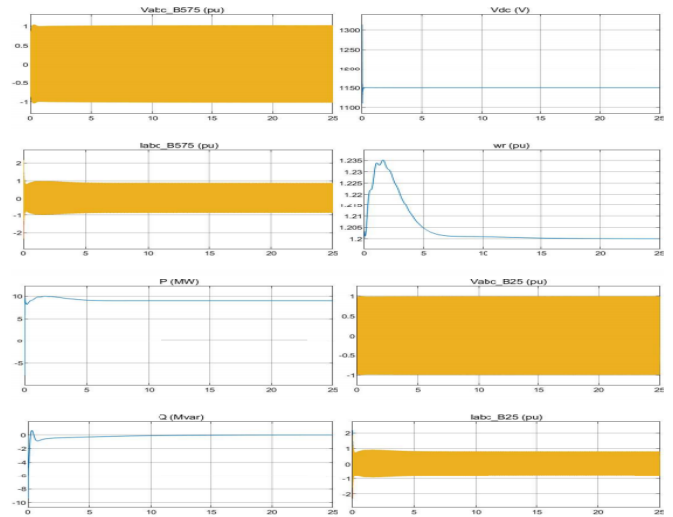


**Fig. 7.** DFIG wind farm in normal operating conditions

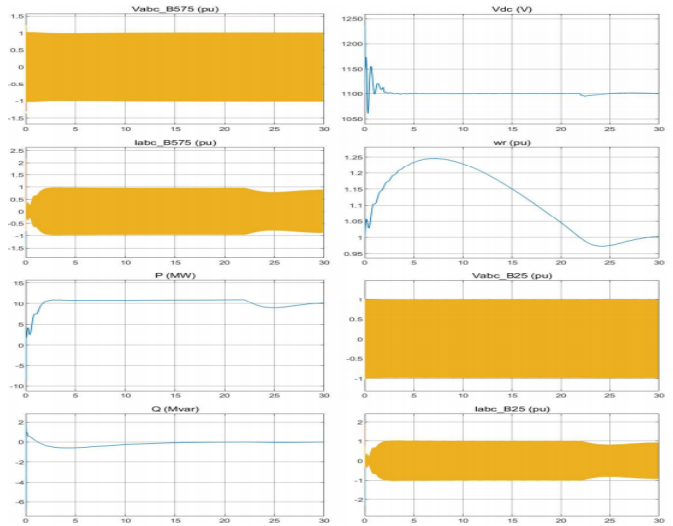


**Fig. 8.** PMSG wind farm in normal operating conditions

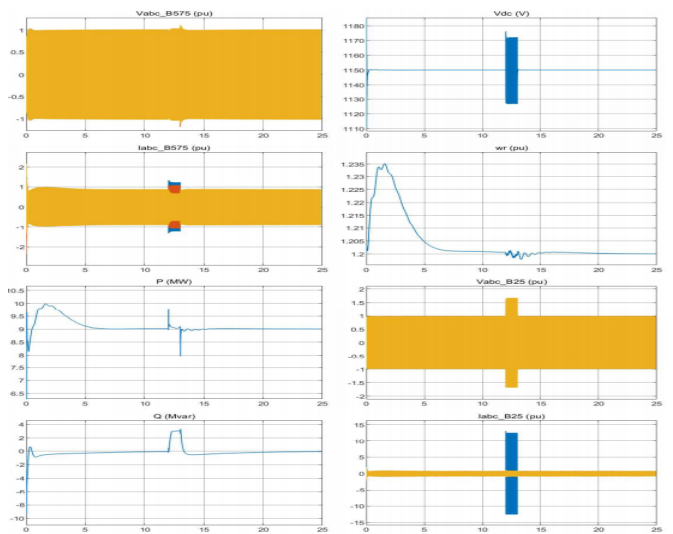


**Fig. 9.** DFIG wind farm with Phase A – Ground fault

Fig. 11 and Fig. 12 show the behavior of the wind power plants and the grid under the conditions of constant wind speed and phase-phase-earth fault. Under these conditions both wind turbines affect the stability of the grid voltage.

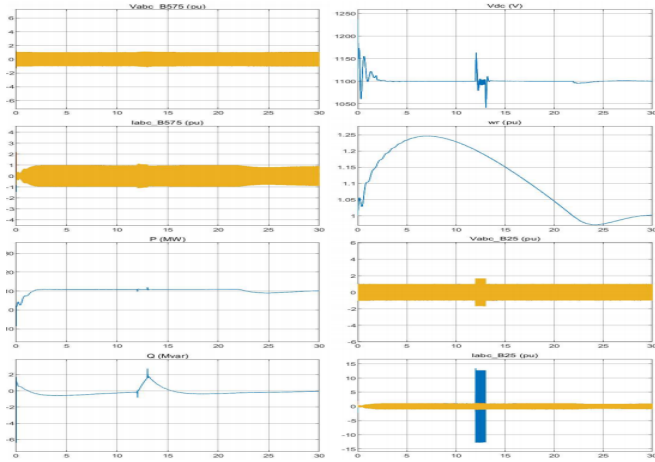


Fig. 10. PMSG wind farm with Phase A – Ground fault

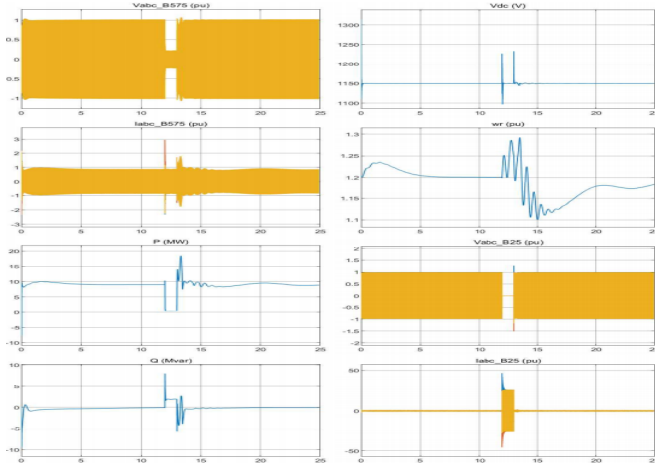


Fig. 11. DFIG wind farm with Phase A – Phase B – Ground fault

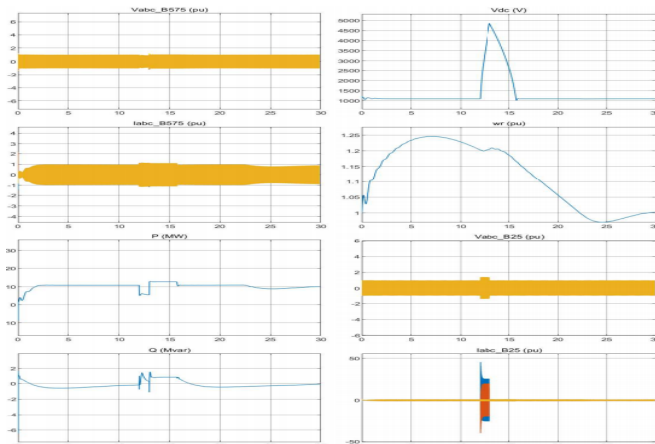


Fig. 12. PMSG wind farm with Phase A – Phase B – Ground fault

Fig. 13 and Fig. 14 show the behavior of the wind power plants and the grid under the conditions of constant wind speed and 3-phase-earth fault. Under these conditions both wind turbines significantly affect the stability of the grid voltage.

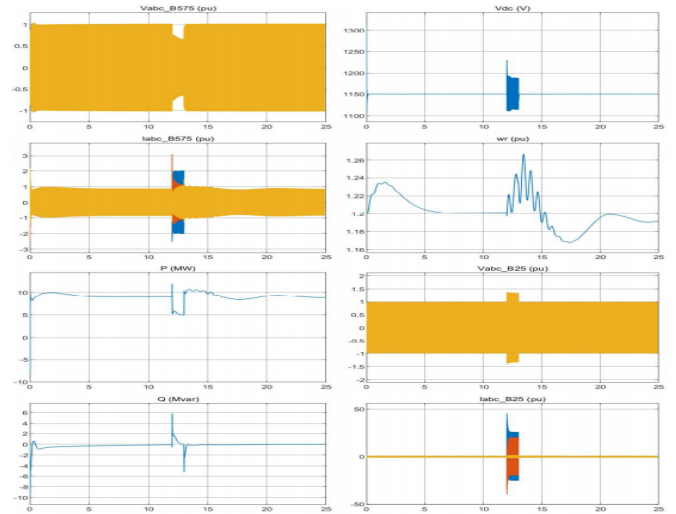


Fig. 13. DFIG wind farm with Phase A – Phase B – Phase C - Ground fault

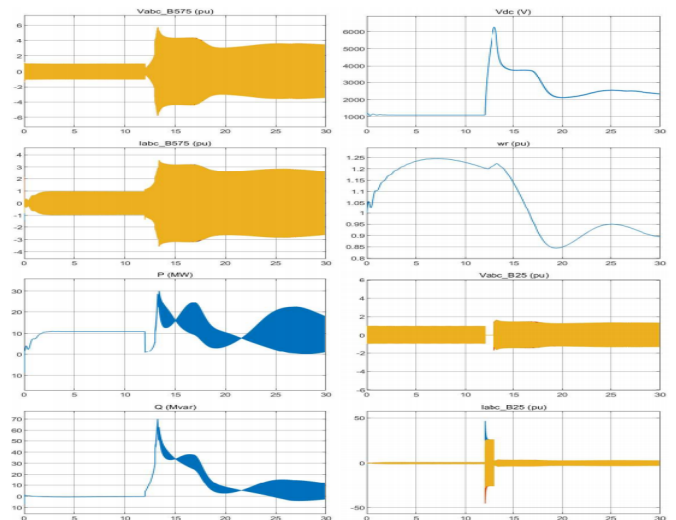


Fig. 14. PMSG wind farm with Phase A - Phase B - Phase C - Ground fault

Fig. 15 and Fig. 16 show the behavior of the wind power plants and the grid under the conditions of constant wind speed and grid voltage drop to 0.5 pu. Under these conditions the DFIG wind turbines are more sensitive to the voltage drop than the PMSG wind turbines. This occurs in the DFIG wind turbines due to the stator leakage flux being divided into natural and forced components. While the natural components rotate synchronously, the forced components remain stationary relative to the stator. In addition, the natural components induce high EMF in the rotor windings, which rises during a voltage drop. In the case of 100% voltage drop at high rotor speed, it reaches its maximum value. As seen in Fig. 15, this situation causes high rotor



currents to flow in the DFIG wind turbines compared to PMSG wind turbines, likely damaging the power electronics circuits and causing an excessive increase of the voltage in the DC link capacitor in both generators. This situation also results in electromagnetic oscillations during the fault.

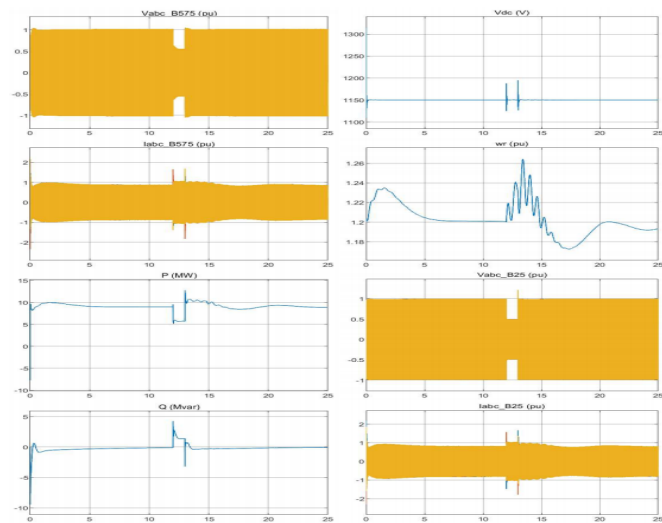


Fig 15. DFIG wind farm with grid voltage drop to 0.5 pu

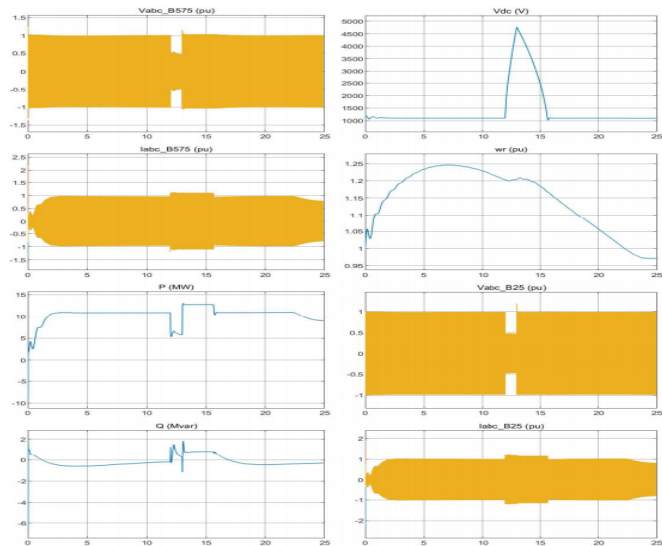


Fig. 16. PMSG wind farm with grid voltage drop to 0.5 pu

The largest oscillations are seen in the DC link voltage for symmetrical errors and in the currents generated in the rotor for asymmetrical (phase-to-phase) faults.

A summary of the comparison between the dynamic responses obtained from the simulations for phase-earth, phase-phase-earth, and three phase-earth short circuit in the DFIG and PMSG wind turbines is given in Table 2 - Table 4. The dynamic response due to voltage drop is given in Table 5.

Table 2. Phase A – Ground fault

Percent oscillation and its duration	DFIG		PMSG	
	% Δ	Time (sec)	% Δ	Time (sec)
$V_{abc_{B575}}$	11	0.4	8	0.8
$I_{abc_{B575}}$	46.6	0.6	22.2	0.6
$P$	11	1,8	20	16
$\Delta Q$	3.2 MVAR	7	2.8 MVAR	16
$V_{dc}$	2.17	1	5.4	16
$w_r$	0.17	8	-	-
$V_{abc_{B25}}$	68	0.2	66	0.1
$I_{abc_{B25}}$	1200	0.2	1200	0.1

Table 3. Phase A – Phase B – Ground fault

Percent oscillation and its duration	DFIG		PMSG	
	% Δ	Time (sec)	% Δ	Time (sec)
$V_{abc_{B575}}$	35	1	20	0.2
$I_{abc_{B575}}$	233	0.9	27.7	12
$P$	44	12	45	17
$\Delta Q$	5.5 MVAR	6	1.5 MVAR	17
$V_{dc}$	7	7	4850-1100	16
$w_r$	5	12	-	-
$V_{abc_{B25}}$	40	0.2	40	0.1
$I_{abc_{B25}}$	4400	0.2	4400	0.1

Table 4. Phase A – Phase B – Phase C - Ground fault

Percent oscillation and its duration	DFIG		PMSG	
	% Δ	Time (sec)	% Δ	Time (sec)
$V_{abc_{B575}}$	80	0.7	5.5-1	-
$I_{abc_{B575}}$	223	10	3.5- 0.9	-
$P$	95	12	30-10	-
$\Delta Q$	8 MVAR	6	70-0	-
$V_{dc}$	7	7	6250-1100	-
$w_r$	7.5	12	-	-
$V_{abc_{B25}}$	50	0.2	1.66-1	-
$I_{abc_{B25}}$	4500	0.2	46-1	-

**Table 5.** Voltage drop condition

Percent oscillation and its duration	DFIG		PMSG	
	% Δ	Time (sec)	% Δ	Time (sec)
$V_{abc_{B575}}$	50	0.6	50	0.2
$I_{abc_{B575}}$	83.3	7	27.2	12
$P$	44.4	12	50	12
$\Delta Q$	4.2 MVar	7	1.8 MVar	6
$V_{dc}$	3.4	1	331.8	3
$w_r$	5	12	-	-
$V_{abc_{B25}}$	50	0.4	50	0.1
$I_{abc_{B25}}$	65	7	20	12

## 6. Discussion

This study investigates the behaviour of PMSG and DFIG wind turbines connected to the grid under the fault conditions of one-phase-ground, two-phase-ground and three-phase-ground short circuits, and the response to a significant voltage drop.

During a three-phase-ground fault, the DC link voltage increases from 1100 V to 6250 V in the PMSG wind turbine. The DC link voltage in the DFIG wind turbine rises from 1150 V to 1230 V under the same conditions. In all other short circuit fault conditions, the behavior of the DFIG wind turbine is similar to that of the PMSG wind turbine for active power and voltage stability. The PMSG wind turbines supplies 50% less reactive power to the grid on average than the DFIG wind turbines. The detail of the magnitude (%) and oscillation time of both systems is shown in tables 2-5. The phasor voltages  $V_{abc_{B575}}$  on the grid-side converter during the voltage drop to 0.5 pu depend on the rating of the DFIG generator and the results from the simulation are shown in Figure 15. The phasor currents  $I_{abc_{B575}}$  flowing into the grid-side converter depend on the rating of PMSG generator and the results from the simulation are shown in Figure 16. The figures show that during the time the voltage drop is applied the PMSG wind turbines have better current stability, with the PMSG wind turbine having a current difference of 27.2%, whereas the DFIG wind turbine has a difference of 83.3%. In contrast, Table 5 shows that there are significant differences in the variations in the DC link voltages, with the DFIG wind turbine DC link voltage being more stabilized than the PMSG wind turbine. Figure 15 shows the DC link voltage of the DFIG wind turbine oscillates due to the voltage drop, however it returns rapidly to its nominal value.

## 7. Conclusion

The simulation results show that systems containing DFIG wind turbines reach the nominal operating values more quickly than systems containing PMSG wind turbines. DFIG wind turbines constantly change the pitch angle to control power so even in constant wind speed the rotor speed may change over time. This makes systems containing DFIG

wind turbines provide power control in a less costly and more efficient manner. At high wind speeds, the pitch controller protects the wind turbine by limiting the maximum output power, while the pitch angle remains constant at low wind speeds. The flexibility in pitch angle provided by DFIG wind turbines reduces the mechanical stress on the blades of the wind turbine caused by the variable wind speed. For this reason, problems such as vibration and flicker in the generated torque are also reduced.

Pitch control can also be used for variable wind speed systems in PMSG wind turbines to control its stator connection with the full scale power converter. Thus, active power and reactive power at the total output can be controlled, but this leads to more transmission and switching losses, as well as increased cost. In addition, PMSGs with full-scale frequency converters are more affected by malfunctions in the network and it is seen that the DC link voltage increases excessively. In contrast, the reactive power generation and consumption features provided by the converters of DFIG technology remove the need for capacitor groups or STATCOM, thus reducing system cost.

## References

- [1] Knudsen, H.Akhmatov, V., (2001), "Evaluation of Flicker Level in a T&D Network with a Large Amount of Dispersed Windmills", 16th International Conference and Exhibition on CIGRE, 18-21 June 2001. (Conference Paper)
- [2] Yongning, C.; Yan, L.; Zhen, L.; Ziyu, C.; Hongzhi, L. "Study on Grid-connected Renewable Energy Grid Code Compliance". In Proceedings of the 2019 IEEE Sustainable Power and Energy Conference (iSPEC), Beijing, China, 21–23; pp. 72–75, November 2019. (Conference Paper)
- [3] Y. Oguz, I. Guney, H. Calik, "Power quality control and design of power converter for variable-speed wind energy conversion system with permanent-magnet synchronous generator", The Scientific World Journal, pp.1-15, 2013. (Article)
- [4] Islam, M.M.; Hossain, E.; Padmanaban, S.; Brice, C.W. "A New Perspective of Wind Power Grid Codes Under Unbalanced and Distorted Grid Conditions", IEEE Access, Vol 8, pp.15931–15944, 2020. (Article)
- [5] Masters, G.M., "Renewable and Efficient Electric Power Systems", John Wiley & Sons, New Jersey. 2004.(Book)
- [6] M. Tsili and S. Papathanassiou, "A review of grid code technical requirements for wind farms ", IET Renew. Power Generator, vol. 3, no. 3, pp. 308 332, Sep. 2009. (Article)
- [7] M. N. I. Sarkar, L. G. Meegahapola, and M. Datta, "Reactive power management in renewable rich power grids: A review of grid-codes, renewable generators, support devices, control strategies and optimization



- algorithms," *IEEE Access*, vol. 6, pp. 41458 41489, 2018. (Article)
- [8] K.-J. Du, X.-Y. Xiao, Y. Wang, Z.-X. Zheng, and C.-S. Li, "Enhancing fault ride-through capability of DFIG-based wind turbines using inductive SFCL with coordinated control," *IEEE Trans. Appl. Supercond.*, vol. 29, no.2, pp.1- 6, Mar. 2019. (Article)
- [9] M. Firouzi and G. B. Gharehpetian, "LVRT performance enhancement of DFIG-based wind farms by capacitive bridge-type fault current limiter," *IEEE Trans. Sustain. Energy*, vol. 9, no. 3, pp. 1118 1125, Jul. 2018. (Article)
- [10] M. Islam, H. A. Mohammadpour, A. Ghaderi, C.W. Brice, and Y.-J. Shin, "Time-frequency-based instantaneous power components for transient disturbances according to IEEE standard 1459 ", *IEEE Trans. Power Del.*, vol. 30, no. 3, pp. 1288 1297, Jun. 2015. (Article)
- [11] R. Duan and F.Wang, "Fault diagnosis of on-load tap-changer in converter transformer based on time frequency vibration analysis", *IEEE Trans. Ind. Electron.*, vol.63, no.6, pp.3815 3823, Jun. 2016. (Article)
- [12] T. Neumann, T. Wijnhoven, G. Deconinck, and I. Erlich, "Enhanced dynamic voltage control of type 4 wind turbines during unbalanced grid faults ", *IEEE Trans. Energy Convers.*, vol.30, no.4, pp.1650 1659, Dec. 2015. (Article)
- [13] Y. Zhang, E. Muljadi, D. Kosterev, and M. Singh, "Wind power plant model validation using synchrophasor measurements at the point of inter- connection", *IEEE Trans. Sustain. Energy*, vol.6, no.3, pp.984 992, Jul. 2015. (Article)
- [14] Technical Analysis of the August 14, 2003, Blackout: What Happened, Why, and What Did We Learn? North Amer. Electr. Rel. Council, Atlanta, GA, USA, Jul. 2014. (Article)
- [15] M. Islam, H. A. Mohammadpour, P. Stone, and Y.-J. Shin, "Time- frequency based power quality analysis of variable speed wind turbine generators," *Int.Proc. IECON 39th Annu. Conf. IEEE Ind. Electron. Soc.*, Nov. 2013. (Conference Paper)
- [16] P. Stone, M. Islam, and Y.-J. Shin, "Power quality impact of wind turbine generators on the electrical grid", *Int.Proc. IEEE Energytech*, Cleveland, OH, USA, pp. 1-6. May 2012. (Conference Paper)
- [17] X. Liu, L. Li, Z. Li, X. Chen, T. Fernando, H. H.-C. Iu, and G. He, "Event-trigger particle filter for smart grids with limited communication bandwidth infrastructure," *IEEE Trans. Smart Grid*, vol.9, no.6, pp. 6918 6928, Nov.2018. (Article)
- [18] P. Kundur, "Definition and classification of power," *IEEE Transactions on Power Systems*, Vol. 19, No. 2, pp.1387 – 1401, 2004. (Article)
- [19] H.Calik, G.Yalcin, E.Sehirli, "Power Factor Correction in Induction Heating System Using PFC Boost Converter", *European Journal of Technique*, Vol.2, pp.464-475, 2020. (Article)
- [20] Abdelkader Harrouz; Ilhami Colak; Korhan Kayisli "Energy Modeling Output of Wind System based on Wind Speed", 2019 8th International Conference on Renewable Energy Research and Applications (ICRERA). (Article)
- [21] Samir Moulahoum, Mohamed Hallouz, Nadir Kabache, Selman Kouadria, Neural Network Based Field Oriented Control for Doubly-Fed Induction Generator, *International Journal of Smart Grid – ijSmart Grid*, Vol 2, No 3 (2018): September, (Article)
- [22] A. Harrouz, I. Colak, and K. Kayisli, "Energy Modeling Output of Wind System based on Wind Speed", 8th International Conference on Renewable Energy Research and Applications (ICRERA), 2019. (Conference Paper)
- [23] E. Ibrahim, "Low Voltage Ride-Through of Permanent Magnet Synchronous Generator Wind Energy Systems", University of Strathclyde, 2014. (Thesis Ph.D.)
- [24] Habib Benbouhenni, Zinelaabidine Boudjema, Abdelkader Belaid, "DFIG-Based WT System Using FPWM Inverter", *International Journal of Smart Grid – ijSmartGrid*, Vol 2, No 3 (2018): September (Conference Paper)